

Construction of Luminescent Gold(I) Aryl Thiolates *via* Isonitrilegold(I) Complexes: Influence of Synthetic Methodology and the Thiolate Ligand on Structure and Properties

Robert E. Bachman^a and Sheri A. Bodolosky-Bettis^b

^a Department of Chemistry, The University of the South, 735 University Avenue, Sewanee, TN, 37383, USA

^b Department of Chemistry, Georgetown University, 37th and O Sts, Washington, DC 20057, USA

Reprint requests to Prof. Robert E. Bachman. Fax: 931-598-1145. E-mail: rbachman@sewanee.edu

Z. Naturforsch. **2009**, *64b*, 1491 – 1499; received October 2, 2009

Dedicated to Professor Hubert Schmidbaur on the occasion of his 75th birthday

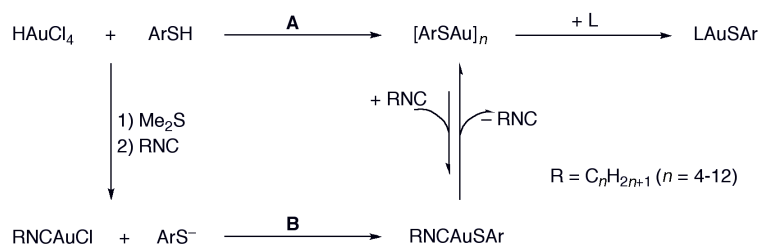
Gold thiolate polymers ($[\text{ArSAu}]_n$) were prepared *via* two synthetic routes – the direct reaction of an aromatic thiolate (ArSH) with HAuCl_4 , or the reaction of an isonitrilegold(I) chloride complex with a thiolate anion. The former route, which is general to almost all thiols, yields an amorphous and non-luminescent material. The latter route, which is more limited in scope, proceeds *via* an isonitrilegold(I) thiolate complex and typically yields a crystalline and luminescent material. Addition of electron-donating groups to the thiol aromatic ring leads to more rapid polymer formation and loss of luminescence while addition of electron-withdrawing groups slows or stops polymer formation and leads to a red-shift of the luminescence of the final polymeric materials. Two isonitrilegold(I) thiolate complexes with varying numbers of fluorine substituents on the thiolate aromatic ring were characterized crystallographically – $\text{C}_8\text{H}_{17}\text{NCAu}(p\text{-FC}_6\text{H}_4\text{S})$ and $\text{C}_{12}\text{H}_{25}\text{NCAu}(2,4\text{-F}_2\text{C}_6\text{H}_3\text{S})$. As the fluorination of the aromatic ring increases, no significant changes were observed in the bond lengths of the complexes; however, the intermolecular Au-S distances lengthen while the aurophilic interaction distances decrease. These results suggest clear relationships between the molecular structure and both the supramolecular structure and photophysical properties in these materials.

Key words: Gold Thiolates, Luminescence, Isonitrile Gold Complexes

Introduction

Gold(I) complexes have attracted significant attention for at least the last two decades due to their unique properties and numerous potential applications [1]. Perhaps the most distinctive feature of these complexes is the ability of gold(I) to form aurophilic interactions [2]. These strong non-covalent interactions have been shown to be capable of stabilizing unusual coordination numbers and geometries around a host of main-group elements [1], of creating unusual supramolecular structures [3] and of inducing novel mesophase behavior in very simple systems [4]. The presence of aurophilic interactions has also been shown to generate, or modify, luminescent behavior in numerous gold-based complexes and materials [5]. Applications for gold complexes continue to be found at an increasing rate and include areas as widespread as hetero- and homogeneous catalysts [6] on the one hand and chemosensors on the other [7].

Gold thiolate complexes are a particularly important class of gold complexes due, in part, to the high affinity of gold for sulfur. In addition to the applications described above, gold thiolates have been utilized commercially in areas as diverse as metallopharmaceuticals [8] and gilding inks [9]. Thiolate ligands are also a mainstay of SAM surface chemistry [10] and gold nanoparticle research [11], areas of significant interest in recent years. Indeed, gold(I) thiolate polymers are a key step in the Brust synthesis of gold nanoparticles [12]. Despite their significant role in the preparation of gold nanoparticles, relatively little is known about the structure and properties of the thiolate polymers themselves. We have previously reported that the supramolecular structure of the gold(I) phenylthiolate polymers can have a dramatic impact on the photophysical properties of these materials [13]. Recently, others have noted similar effects in a variety of gold thiolate-based materials [14]. In our initial work, we also noted that the supramolecular structure of these



Scheme 1. Reactions leading to the formation of [ArSAu]_n polymers and their reaction with two electron donor ligands.

polymeric materials could be, at least partially, controlled by the method of synthesis and/or post synthesis treatment. In this study we explore the generality of our synthetic methodology and probe the relationship between the structure of the thiolate and the supramolecular structure and photophysical properties for the resulting polymeric materials.

Results and Discussion

As we have previously reported [13], the polymeric species [PhSAu]_n can be prepared by either direct reaction of thiophenol with HAuCl₄ or by reaction of isonitrile gold(I) complexes, RNCAuCl, with the corresponding anionic thiolate. The latter reaction proceeds *via* initial substitution of the anionic ligand at gold followed by loss of the relatively labile isonitrile ligand (Scheme 1). These different routes produced materials of identical elemental composition but dramatically different physical properties. For the direct reaction (route A), the resulting polymeric material is amorphous and non-luminescent, while use of the isonitrile complex as a synthon (route B) generates a highly crystalline and luminescent product. In this work, we have sought to explore the generality of these reactions with respect to the identity of the thiolate and the ancillary ligand. Additionally, we sought to determine the impact of the thiolate identity on the photophysical properties of the gold thiolate polymers.

Gold(I) thiolate polymers, [ArSAu]_n, can be prepared by direct reaction of essentially any aryl thiol with HAuCl₄ (Table 1). Notable exceptions are highly fluorinated systems, such as HC₆F₄SH and C₆F₅SH, which yield stable gold(III) complexes [15], and *t*-BuC₆H₄SH, which produces a soluble oligomeric material [16].

As with the thiophenol, the resulting solids typically show XRD patterns (Fig. 1) consistent with an amorphous material. While these patterns are relatively featureless, the low angle peak can be correlated with the distance expected for a layered structure such as

Table 1. Synthetic Routes to Gold Thiolate Polymers and Outcomes From These Reactions.

Thiol	Route	Form	Luminescent?
PhSH	A	amorphous	N
	B	crystalline	Y
<i>p</i> -FC ₆ H ₄ SH	A	amorphous	N
	B	crystalline	Y
2,4-F ₂ C ₆ H ₃ SH	A	amorphous	N
	B	isonitrile complex	
<i>o</i> -CO ₂ HC ₆ H ₃ SH	A	amorphous	N
	B	crystalline	Y
<i>p</i> -CH ₃ C ₆ H ₃ SH	A	amorphous	N
	B	partially crystalline	N
<i>p</i> -CH ₃ OC ₆ H ₃ SH	A	amorphous	N
	B	partially crystalline	N
<i>t</i> -BuC ₆ H ₃ SH	A / B	soluble oligomer	N

that shown in Fig. 1 assuming a slight tilt of the polymer chain direction relative to the layer direction. The agreement between this diffraction peak and the expectation based on the model structure improves significantly (see Fig. 2 below) for crystalline samples, providing confidence in the correctness of the model. The broad features at higher angle are consistent with expectations for in-layer Au–Au, π – π and Au–S contacts.

In contrast, use of the isonitrilegold(I) chloride complexes as a synthon for the production of crystalline gold thiolate polymers proved to be of more limited scope. Complexes prepared using thiolate ligands containing more than one fluorine atom failed to lose the isonitrile ligand, even after prolonged reaction times and/or heating under reduced pressure. Rather, the isonitrile complexes were isolated in good to excellent yield by simply evaporating the reaction solvent. Interestingly, the presence of a single carboxylate group seems to provide a situation intermediate between one and two fluorine substituents. In this case, the loss of the isonitrile ligand occurs, albeit at a very slow rate. In contrast, the use of aryl thiolates with electron-donating groups (CH₃, *t*-Bu, OCH₃) in the *para* position results in rapid loss of the isonitrile ligand from the RNCAuSAr complex; however, the resulting ma-

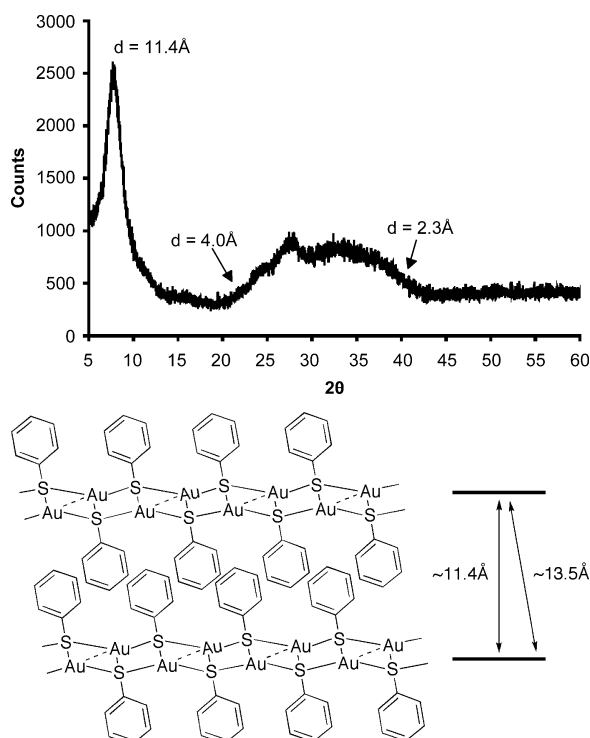


Fig. 1. *Top*: XRD of amorphous $[\text{PhSAu}]_n$ prepared from HAuCl_4 and PhSH . *Bottom*: Model of a layered structure consistent with the observed XRD pattern.

materials are less crystalline than the parent material and show no luminescence.

In those systems where it occurs, the rate of isonitrile loss was also observed to be dependent on the molecular mass of the isonitrile ligand, with heavier (longer alkyl chain) ligands dissociating more slowly. This kinetic stability has allowed us to crystallize several examples of the RNCAuSAr complexes when R contains at least five carbon atoms. These crystal structures, to be discussed below, provide significant insight into the potential aggregation motifs in these systems and, consequently, the structural requirements for generating luminescent materials. However, it is worth noting that crystalline materials with appropriate thiolate ligands (for example, $\text{Ar} = \text{Ph}$, $p\text{-FC}_6\text{H}_4$) slowly convert to $[\text{ArSAu}]_n$ *via* loss of the isonitrile ligand, as seen previously [12].

These synthetic results highlight several important points. First, the dependence of the rate of the second step of route B on the molecular mass of the isonitrile ligand suggests that the loss of the isonitrile to form $[\text{ArSAu}]_n$ is an equilibrium process ultimately driven by LeChâtelier's principle *via* loss of the isonitrile to

the vapor phase. This observation is consistent with the relatively greater stability for the complexes prepared by Schmidbaur and others based on bulky, and hence non-volatile, isonitrile ligands [14b, 17].

The reversibility of the isonitrile complexation reaction allows for the conversion of non-luminescent, amorphous samples of selected $[\text{ArSAu}]_n$ materials into their luminescent, crystalline forms *via* treatment with a catalytic amount of an isonitrile (typically ≤ 5 mol-% of $n\text{-BuNC}$). As we noted previously [12], this amorphous to crystalline treatment can be effected, although not in a synthetically useful way, by heating the amorphous material strongly. For example, heating $[\text{PhSAu}]_n$ to just below its decomposition temperature (~ 230 °C) results in an exothermic phase transition [13]. This behavior suggests that transformation from the amorphous to the crystalline state is enthalpically favored, and the initial amorphous state found in route A is the result of kinetic factors. Consequently, it seems reasonable that the catalytic isonitrile plays the role of a transport agent, dissolving “high energy” amorphous monomers (or oligomers) and depositing them onto “low energy” growing crystalline polymers. If this model is correct, it suggests a potential method for controlling the internal structure of gold thiolate polymers prior to their reduction to gold nanoparticles, and hence, a potential way to control structure in gold nanoparticles.

This catalytic conversion process is most effective when $\text{Ar} = \text{Ph}$ or $p\text{-FC}_6\text{H}_4$. For materials with electron-donating groups, such as $[p\text{-CH}_3\text{C}_6\text{H}_4\text{SAu}]_n$, catalytic treatment with RNC does enhance the crystallinity of the material, particularly in the low-angle region (Fig. 2), but does not produce the characteristic intense orange-red luminescence seen in the other materials. These results suggest that the ordering of gold-sulfur moieties, and the formation of extended Au–S and Au–Au contacts within the layer, are critical for producing luminescent behavior. In contrast, attempts at catalytic modification of highly fluorinated polymers, such as $[2,4\text{-F}_2\text{C}_6\text{H}_3\text{SAu}]_n$, result in dissolution of the polymer *via* complex formation with the added isonitrile. Indeed, addition of a stoichiometric amount of $\text{C}_8\text{H}_{17}\text{NC}$ to a sample of $[2,4\text{-F}_2\text{C}_6\text{H}_3\text{SAu}]_n$ prepared by route A led to quantitative dissolution of the starting polymer and isolation of $\text{C}_8\text{H}_{17}\text{NCAuSAr}$ as X-ray-quality crystals in good yield. Similarly, reaction of any polymeric material with a non-volatile donor, such as Ph_3P , results in dissolution of the polymer and generation of LAuSAr complexes (Scheme 1).

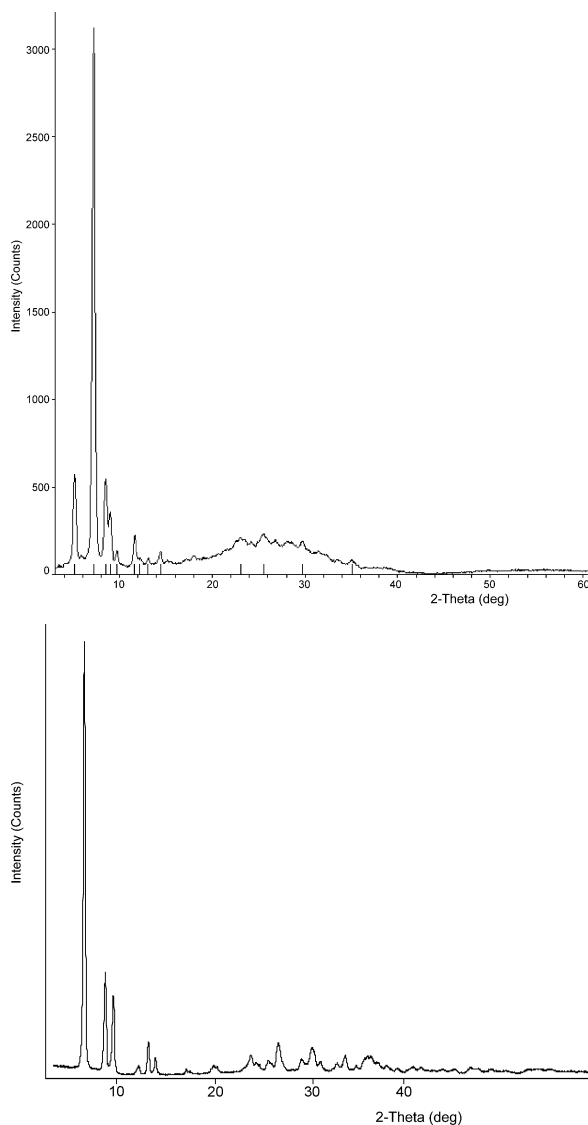


Fig. 2. *Top*: XRD pattern of $[p\text{-CH}_3\text{C}_6\text{H}_3\text{SAu}]_n$ after catalytic treatment with BuNC. *Bottom*: XRD Pattern of $[\text{PhSAu}]_n$ after the same treatment. Note significantly higher degree of crystallinity in the latter case in the high-angle region.

The exquisite sensitivity of the reaction outcome to the thiolate ligand's electronic and steric structure is also striking. As the electron density at sulfur is lowered by the addition of electron-withdrawing groups to the aromatic ring, the lability of the isonitrile ligand decreases dramatically, such that RNCAuSAr is favored over $[\text{ArSAu}]_n$. Interestingly, this trend mirrors our observation that strongly electron-deficient thiolates can form gold(III) complexes rather than affect-

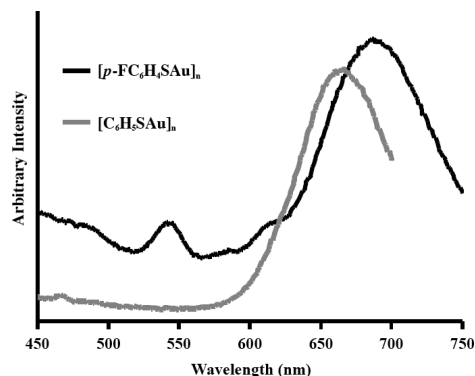


Fig. 3. The emission spectra for $[p\text{-FC}_6\text{H}_4\text{SAu}]_n$ (black line) and $[\text{PhSAu}]_n$ (grey line).

ing reduction to gold(I) [15]. Additionally, the inability of the thiolate ligands containing even slightly bulky substituents (*e. g.*, $p\text{-CH}_3$) to form luminescent materials illustrates the sensitivity of the supramolecular structure to small steric changes, even in the periphery of the ligands. It is also possible that the increased electron-density in these thiolate ligands increases the rate of ligand dissociation enough that the formation of amorphous material is even more kinetically favored, which might also be expected to hinder the effectiveness of isonitriles as recrystallization agents.

Crystalline polymer samples of $[\text{PhSAu}]_n$, $[p\text{-FC}_6\text{H}_4\text{SAu}]_n$ and $[o\text{-CO}_2\text{HC}_6\text{H}_4\text{SAu}]_n$, prepared *via* either route B or catalytic treatment of an amorphous sample of these materials produced in route A, showed an intense orange luminescence. Addition of an electron-withdrawing group in $[p\text{-FC}_6\text{H}_4\text{SAu}]_n$ and $[o\text{-CO}_2\text{HC}_6\text{H}_4\text{SAu}]_n$ results in a small red-shift (47 nm) in the luminescence wavelength from 643 nm for $[\text{PhSAu}]_n$ to 690 nm for $[p\text{-FC}_6\text{H}_4\text{SAu}]_n$ and $[o\text{-CO}_2\text{HC}_6\text{H}_4\text{SAu}]_n$ (Fig. 3). Based on their long (~ 5 ns) lifetimes, we [13] as well as others [18] have previously assigned this low-energy emission as arising from a metal-centered triplet state. The observed red-shift seems to indicate that the presence of electron-withdrawing groups stabilizes the ligand-to-metal charge transfer excited state slightly.

The solid-state structure of $[\text{C}_8\text{H}_{17}\text{NCAu}(p\text{-FC}_6\text{H}_4\text{S})]$ (Fig. 4) is essentially identical to those we have previously reported for RNCAuSPh ($\text{R} = \text{C}_5\text{H}_{11}$ and C_7H_{13}) [13], with all the molecular bonding parameters (Table 2) in agreement with expectations. The supramolecular structure of these three systems is also essentially identical, consisting of a “crinkled tape” motif made up by aurophilic interactions and

	Intramolecular bond lengths (Å)			
	Au–S	Au–C	C–N	S–C _{Ar}
C ₅ H ₁₁ NCAuSPh	2.272(2)	1.967(10)	1.144(1)	1.772(7)
C ₇ H ₁₃ NCAuSPh	2.274(17)	1.978(7)	1.136(8)	1.781(5)
C ₈ H ₁₇ NCAuSC ₆ H ₄ F- <i>p</i>	2.270(2)	1.985(7)	1.121(8)	1.775(6)
C ₈ H ₁₇ NCAuSC ₆ H ₃ F ₂ -2,4	2.273(1)	1.970(4)	1.132(5)	1.770(4)
	Intermolecular contacts (Å)			
	Au...Au	Au...S _{short}	Au...S _{long}	
C ₅ H ₁₁ NCAuSPh	3.786(1)	3.663(2)	4.022(2)	
C ₇ H ₁₃ NCAuSPh	3.611(1)	3.686(2)	4.060(2)	
C ₈ H ₁₇ NCAuSC ₆ H ₄ F- <i>p</i>	3.569(1)	3.709(2)	4.018(2)	
C ₈ H ₁₇ NCAuSC ₆ H ₃ F ₂ -2,4	3.409(1)	4.047(1)	–	

Table 2. Significant bond lengths and intermolecular contacts.

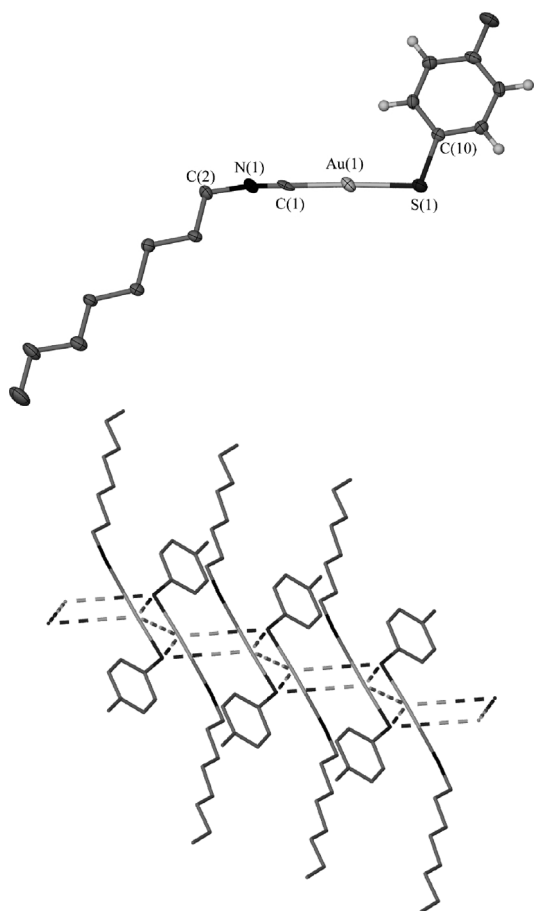


Fig. 4. *Top*: View of an individual molecule of C₈H₁₇NCAu(*p*-FC₆H₄S) showing the linear coordination geometry at gold. *Bottom*: A view of the “crinkled tape” motif formed *via* Au–S and Au–Au interactions.

Au–S contacts (see Table 2). Given the pattern of short and long Au–S contacts, the tape motif can be thought of as arising in two distinct stages. The first is the formation of dimeric units *via* two Au–S contacts and one aurophilic interaction, while the second is

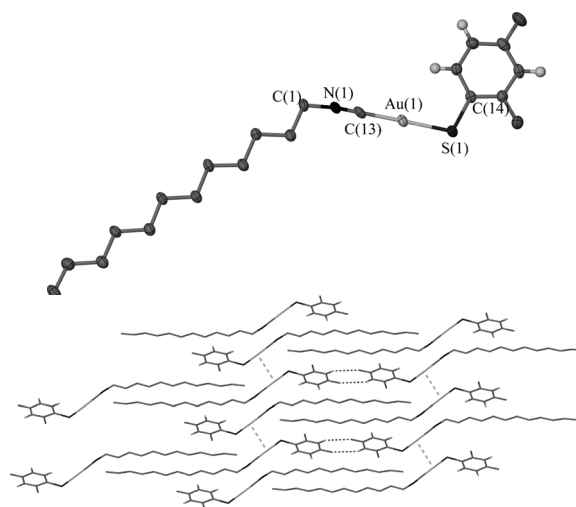


Fig. 5. *Top*: View of one molecule of C₁₂H₂₅NCAu(2,4-F₂C₆H₃S) showing the overall molecular geometry. *Bottom*: View of the major intermolecular interactions, Au–Au and C–H...F hydrogen bonding, responsible for the supramolecular structure in this system.

the aggregation of these dimers through longer, and presumably weaker, Au–S contacts.

The structure of the related difluoro complex, [C₁₂H₂₅NCAu(2,4-F₂C₆H₃S)], (Fig. 5) is similar to the other complexes at the molecular level; however, it is markedly different at the supramolecular scale. In this case, the molecules are again organized into discrete dimers *via* a pair of Au–S contacts and a single aurophilic interaction. However, these dimers then aggregate not through further Au–S contacts but through a pair of complementary C–H...F hydrogen bonds involving the *para* fluorine on one ring interacting with the fairly acidic hydrogen at the 3-position (*i. e.*, between the two fluorine atoms). The observed H–F distance of 2.78 Å is comparable to those seen previously, which range from 2.36 to 2.86 Å. It is worth noting that while C–H...F interactions are weaker than classical

hydrogen bonds, they have been found to make a significant contribution to packing of the molecules [19]. The significant alteration of the supramolecular structure seen from the seemingly minor change in molecular structure from one fluorine atom to two is a stark example of the subtle balance of forces responsible for packing in the solid state.

Given the constancy of the packing seen in systems that yield luminescent materials, and the inability to form luminescent material from an alternative packing arrangement, it seems reasonable to conclude that the aggregation motif plays an important role in the physical properties of the final polymeric material. We have previously suggested a mechanism for the formation of the luminescent forms of these polymers involving the self-assembly of the isonitrile complexes into the motif seen in Fig. 4 followed by loss of the isonitrile ligands to yield a ladder polymer structure [13]. The results of this current work are completely consistent with this conjecture; when the “crinkled tape” can form, luminescent materials result, and when steric factors or other intermolecular interactions disrupt this packing motif, non-luminescent materials result. For example, the inability of the complexes with electron-donating groups, such as RNCAu(*p*-CH₃C₆H₄S), is a result of the steric cost of the substitution of a hydrogen atom for a significantly larger group such as methyl or methoxy. The presence of bulky groups at the aromatic ring generates a curvature to a growing thiolate oligomer. When the curvature is large enough, as in the *t*-Bu case, the result is the formation of a small oligomer with a ring structure. This idea is supported by the solubility of gold thiolate samples made from *t*-BuC₆H₄S(H) regardless of synthetic route [16].

The intermolecular contacts present in these closely related structures also present an interesting trend (Table 2), particularly given the constancy of the bond lengths between complexes. As the number of fluorine atoms increases, the short intradimer Au–S contact lengthens, and the aurophilic contact shortens. Hence, it appears that the decrease in electron density at sulfur from the addition of strongly electron-withdrawing groups on the aromatic ring results in weaker Au–S interactions and concomitantly stabilize the aurophilic interaction. These structural findings fit well with our interpretation of the luminescence data above.

Conclusion

Through this work we have elaborated on our initial findings, showing that sterically unencumbered la-

bile ligands, such as isonitriles, can be used to control the solid-state structure of gold thiolate polymers, in at least some cases. Moreover, we have shown that the electronic structure of the aromatic ring can be used to tune the photophysical behavior of these novel luminescent materials. Lastly, we have again demonstrated how the delicate interplay of forces such as hydrogen bonding, metal-ligand interactions and aurophilic interactions can generate surprising shifts in a solid-state structure.

Experimental Section

General Information

Experiments were carried out in air unless otherwise noted. Unless stated otherwise, all starting materials were available commercially and used as received from the vendor. Isonitrile complexes of gold(I)chloride, RNCAuCl (R = *n*-alkyl), [Et₄N][Au(SC₆F₄H)₂] and Me₂SAuCl were synthesized *via* literature procedures [4, 15, 20].

¹H, ¹⁹F, and ³¹P{¹H} NMR spectra were recorded on a Varian 300 spectrometer using the solvents specified. The ¹H chemical shifts were internally referenced to TMS (δ = 0 ppm). ¹⁹F NMR spectra were externally referenced to trifluoroacetic acid (δ = 0 ppm). ³¹P{¹H} NMR spectra were generally externally referenced to phosphoric acid (δ = 0 ppm) or triphenyl phosphate (0.0485 M, δ = –17.1 ppm). Infrared spectra were recorded using neat solids on a Perkin Elmer Spectrum One FT-IR spectrometer *via* an ATR attachment. Fluorescence spectra were recorded on a FluoroMax-2 spectrophotometer. All differential scanning calorimetry (DSC) measurements were obtained using open aluminum pans on a TA Instruments 2910 modulated DSC.

Synthesis of [SC₆H₅Au]_n

Method 1

Benzenethiol (2 mL, 19.5 mmol) was added dropwise to a solution of H₂AuCl₄ · H₂O (1.60 g, 4.71 mmol) in EtOH (30 mL). The mixture was left to stir for 30 min, during which time a white precipitate formed, and the solution turned from yellow to colorless. The solid was isolated by filtration, washed with EtOH and ether, and dried in air. Yield: 1.24 g (86 %). – Anal. for C₆H₅SAu: calcd. C 23.54, H 1.65; found C 23.47, H 1.54. – IR: ν = 1586, 1484, 1033, 739, and 491 cm^{–1}. This material shows no luminescence.

Method 2

A solution of benzenethiol (0.035 mL, 0.34 mmol) and KOH (19 mg, 0.34 mmol) in MeOH (5 mL) was added dropwise to a suspension of Me₂SAuCl (100 mg, 0.34 mmol)

in MeOH (10 mL), producing a pale-yellow solid. The mixture was stirred for 2 h. The solid was isolated by filtration, washed with MeOH and ether, and dried in air. Yield: 0.094 g (90 %). – IR: $\nu = 1586, 1484, 1033, 739, 491 \text{ cm}^{-1}$.

Method 3

Benzenethiol (0.034 mL, 0.34 mmol) and KOH (19 mg, 0.34 mmol) were dissolved in MeOH (5 mL). This solution was slowly added to a solution of $\text{C}_2\text{H}_5\text{NCAuCl}$ (97 mg, 0.34 mmol) in MeOH (10 mL), immediately generating a colorless precipitate, which was isolated by filtration. The solid was washed with MeOH and ether and dried in air. Yield: 0.084 g (82 %). Similar results were obtained using $\text{C}_7\text{H}_{13}\text{NCAuCl}$ and $\text{C}_5\text{H}_{11}\text{NCAuCl}$. – Anal. for $\text{C}_6\text{H}_5\text{SAu}$: calcd. Au 64.34, C 23.54, H 1.65; found Au 64.14, C 23.67, H 1.57. – M. p. 168–172 °C (dec). – IR: $\nu = 1586, 1484, 1032, 739, 490 \text{ cm}^{-1}$. – Luminescence: $\lambda_{\text{em}} = 464, 643 \text{ nm}$ with $\lambda_{\text{ex}} = 350 \text{ nm}$.

Synthesis of $[p\text{-FC}_6\text{H}_4\text{SAu}]_n$

Method 1

4-Fluorobenzenethiol (0.872 mL, 8.19 mmol) was added dropwise to a solution of $\text{HAuCl}_4 \cdot \text{H}_2\text{O}$ (0.139 g, 0.409 mmol) in EtOH (20 mL). The mixture was left to stir until a colorless precipitate formed and the solution turned colorless. The solid was isolated by filtration and washed with MeOH and ether and was dried in air. Yield: 0.120 g (91 %). – Anal. for $\text{C}_6\text{H}_4\text{FSAu}$: calcd. C 22.23, H 1.24; found C 22.94, H 1.21. No luminescence was observed in these samples.

Method 2

A solution of 4-fluorobenzenethiol (0.035 mL, 0.33 mmol) and KOH (0.019 g, 0.33 mmol) in MeOH was prepared and added dropwise to a solution of $\text{C}_4\text{H}_9\text{NCAuCl}$ (0.141 g, 0.331 mmol) in MeOH. The mixture was left to stir for ~ 30 min during which time a colorless precipitate formed. The solid was isolated by filtration, washed with MeOH and ether and dried in air. Yield: 0.102 g (95 %). – Anal. for $\text{C}_6\text{H}_4\text{FSAu}$: calcd. C 22.23, H 1.24; found C 21.48; H 1.01. – Luminescence: $\lambda_{\text{em}} = 450, 550, 690 \text{ nm}$ with $\lambda_{\text{ex}} = 330 \text{ nm}$.

Synthesis of $[2,4\text{-F}_2\text{C}_6\text{H}_3\text{SAu}]_n$

2,4-Difluorobenzenethiol (1.29 mL, 2.30 mmol) was added dropwise to a solution of $\text{HAuCl}_4 \cdot \text{H}_2\text{O}$ (0.260 g, 0.767 mmol) in EtOH. The solution was left to stir for approximately 2 h. The colorless precipitate that formed was isolated by filtration, washed with EtOH and ether and dried under suction. Yield: 0.235 g (90 %). – Anal.

for $\text{C}_6\text{H}_3\text{F}_2\text{SAu}$: calcd. C 21.06, H 0.88; found C 20.61, H 0.78. – M. p. 178–180 °C (dec.).

Synthesis of $[p\text{-CH}_3\text{C}_6\text{H}_4\text{SAu}]_n$

Method 1

4-Methylbenzenethiol (0.932 g, 7.52 mmol) was added as a solid to a solution of $\text{HAuCl}_4 \cdot \text{H}_2\text{O}$ (0.128 g, 0.376 mmol) in EtOH. The resulting colorless precipitate was isolated by filtration, washed with EtOH and dried in air. Yield: 0.095 g (79 %). – Anal. for $\text{C}_7\text{H}_7\text{SAu}$: calcd. C 26.26, H 2.20; found C 26.56, H 2.10. – M. p. 190–195 °C (dec.).

Method 2

A solution of 4-methylbenzenethiol (21 mg, 0.17 mmol) and KOH (10 mg, 0.17 mmol) in MeOH was prepared and added dropwise to a solution of $\text{C}_4\text{H}_9\text{NCAuCl}$ (55 mg, 0.17 mmol) in MeOH, resulting in the formation of a colorless precipitate. After 1 h, the solid was isolated by filtration, washed with MeOH and ether and dried in air. Yield: 21 mg (38 %). – Anal. for $\text{C}_7\text{H}_7\text{SAu}$: calcd. C 26.26, H 2.20; found C 26.25, H 2.00. – M. p. 189–193 °C (dec.).

Synthesis of $[p\text{-}t\text{-BuC}_6\text{H}_4\text{SAu}]_n$

To a solution of $\text{HAuCl}_4 \cdot \text{H}_2\text{O}$ (0.100 g, 0.294 mmol) in EtOH, *t*-butylbenzenethiol (0.494 mL, 2.94 mmol) was added. The resulting pale-yellow solid was isolated by filtration and washed with ether and dried in air. – $^1\text{H NMR}$ (CDCl_3): $\delta = 1.16$ (s), 1.30 (s), 1.32 (s), 6.90 (d), 7.27 (m), 7.52 (d), 7.59 (d), 7.68 (d).

Synthesis of $[p\text{-CH}_3\text{OC}_6\text{H}_4\text{SAu}]_n$

Method 1

4-Methoxybenzenethiol (0.282 mL, 2.30 mmol) was added dropwise to a solution of $\text{HAuCl}_4 \cdot \text{H}_2\text{O}$ (0.156 g, 0.459 mmol) in EtOH (20 mL). After 30 min, the resulting colorless solid was isolated by filtration, washed with MeOH and ether, and dried in air. Yield 0.108 g (70 %). – Anal. for $\text{C}_7\text{H}_7\text{OSAu}$: calcd. C 25.01, H 2.10; found C 25.11, H 2.09. – M. p. 192–196 °C (dec.).

Method 2

A solution of 4-methoxybenzenethiol (20 mg, 0.16 mmol) and KOH (9 mg, 0.2 mmol) in MeOH was prepared and added dropwise to a solution of $\text{C}_4\text{H}_9\text{NCAuCl}$ (51 mg, 0.16 mmol) in MeOH. The mixture was left to stir for 1 h during which time a colorless precipitate formed. The solid was isolated by filtration, washed with MeOH and ether, and dried in air. Yield: 0.034 g (62 %). – Anal. for $\text{C}_7\text{H}_7\text{OSAu}$: calcd. C 25.01, H 2.10; found C 24.88, H 1.98. – M. p. 191–194 °C (dec.).

Synthesis of [o-CO₂HC₆H₅SAu]_n

Thiosalicylic acid (0.500 g, 3 mmol) was added as a solid to a solution of HAuCl₄ · H₂O (0.201 g, 0.592 mmol) in EtOH. The solution was allowed to stir for at least 1 h before isolating the resulting pale-yellow solid by filtration. The solid was washed with ether and air-dried. Yield: 0.197 g (95 %). – Anal. for C₇H₅O₂SAu: calcd. C 24.00, H 1.44; found C 23.99, H 1.66. – M. p. 260–265 °C (dec.). – IR: ν = 3384 (broad), 2916, 2847, and 1667 cm⁻¹. – Luminescence: λ_{em} = 470, 690 nm with λ_{ex} = 350 nm.

Synthesis of [(C₈H₇NC)Au(p-FC₆H₄S)]

A solution of 4-fluorobenzenethiol (0.013 mL, 0.13 mmol) and KOH (0.007 g, 0.1 mmol) was prepared in MeOH and was slowly added to a solution of *n*-octylisonitrile gold(I) chloride (0.054 g, 0.13 mmol) in MeOH. The resulting solution was left to stir for ~ 30 min, during which time a cream-colored solid precipitated. The solid was isolated by filtration and washed with MeOH and ether. Yield: 0.023 g (35 %). X-Ray-quality crystals were grown by placing the mother liquor in the freezer for approximately 1 week. – IR: ν = 3089, 3061, 2856, 2246, 1873, 1585, 1481, 1395 cm⁻¹.

Synthesis of [C₁₂H₂₅NCAu(2,4-F₂C₆H₃S)]

A solution of 2,4-difluorobenzenethiol (0.018 mL, 0.16 mmol) and KOH (0.009 g, 0.2 mmol) in MeOH was added to a solution of *n*-dodecylisonitrile gold (I) chloride (0.050 g, 0.16 mmol) in MeOH. Upon stirring, the solution remained transparent and colorless. The solvent was removed *in vacuo* and a pasty colorless solid remained. Yield: 0.036 g (53 %).

X-Ray crystallography and diffraction

Single crystal X-ray data were collected on a Bruker-AXS SMART CCD system equipped with a Bruker-AXS LT2 low temperature device, using graphite-monochromatized MoK α radiation (λ = 0.71073 Å). Initial unit cells were determined using least-squares analysis of a random set of reflections collected from three series of 0.3° wide ω scans (20 frames/series) well distributed in reciprocal space. The intensity data were then collected with 0.3° wide ω scans and a crystal-to-detector distance of 5.0 cm, providing a complete sphere of data to a maximum resolution of approximately 0.75 Å ($2\theta_{max}$ = 56.6°). The data were corrected for Lorentz and polarization effects as well as absorption. An empirical absorption correction was made on the basis of equivalent reflection measurements using Blessing's method as incorporated into the program SADABS [21]. Structure solution and visualization was carried out with the SHELXTL and X-SEED software packages [22, 23]. The structures were

Table 3. Crystal structure data for C₈H₁₇NCAu(*p*-FC₆H₄S) and C₁₂H₂₅NCAu(2,4-F₂C₆H₃S).

	C ₈ H ₁₇ NCAu- (<i>p</i> -FC ₆ H ₄ S)	C ₁₂ H ₂₅ NCAu- (2,4-F ₂ C ₆ H ₃ S)
Formula	C ₁₅ H ₂₁ AuNSF	C ₁₉ H ₂₈ AuNSF ₂
<i>M_r</i>	463.35	537.47
Crystal size, mm ³	0.5 × 0.18 × 0.04	0.56 × 0.44 × 0.08
Crystal system	monoclinic	monoclinic
Space group	<i>C</i> 2/ <i>c</i>	<i>P</i> 2 ₁ / <i>n</i>
<i>a</i> , Å	14.189(3)	16.944(8)
<i>b</i> , Å	5.4178(10)	7.5452(10)
<i>c</i> , Å	41.909(8)	17.936(2)
β , deg	91.419(3)	117.747(2)
<i>V</i> , Å ³	3220.6(10)	2029.5(5)
<i>Z</i>	8	4
<i>D</i> _{calcd} , g cm ⁻³	1.91	1.76
μ (MoK α), cm ⁻¹	92.6	73.7
<i>F</i> (000), e	1776	1048
<i>hkl</i> range	±18, ±6, ±53	±21, ±9, ±22
((<i>sin</i> θ)/ λ) _{max} , Å ⁻¹	0.589	0.589
Refl. measured	15835	20777
Refl. unique / <i>R</i> _{int}	3515 / 0.0522	4422 / 0.0537
Param. refined	174	219
<i>R</i> (<i>F</i>)/ <i>wR</i> (<i>F</i> ²) (all refl.)	0.0431/0.0828	0.0408/0.0639
GoF (<i>F</i> ²)	1.229	1.007
$\Delta\rho_{min}$ (max / min), e Å ⁻³	1.00 / -2.54	0.92 / -1.05

both solved *via* Direct Methods, which allowed essentially all non-hydrogen atomic positions to be assigned. The remaining non-hydrogen atoms were located in the difference map during refinement. All non-hydrogen atoms were refined anisotropically. While the hydrogen atoms could be located in the final difference maps, refinement of these atoms proved unstable. Hence, the hydrogen atoms were included in the final model using a standard riding model. The differences in the hydrogen atom positions in these two models were found to be negligible. Final crystallographic details are summarized in Table 3.

CCDC 753256 and 753257 contain the supplementary crystallographic data for this paper. These data can be obtained free of charge from The Cambridge Crystallographic Data Centre *via* www.ccdc.cam.ac.uk/data_request/cif.

X-Ray powder diffraction experiments were performed on a Rigaku R-Axis Rapid diffractometer equipped with an image plate detector. Graphite-monochromatized CuK α radiation (λ = 1.5419 Å) was used throughout. The samples were mounted onto the goniometer head in 0.1 mm glass capillaries. A CCD microscope camera was used to position the desired region of the sample in the X-ray beam and align it approximately perpendicular to the beam. The plate images were converted to standard *I* vs. 2θ plots using the integration software included with the instrument, and the data were analyzed with JADE 5 PATTERN processing software. Background corrections were made by manual subtraction of the XRD pattern obtained from an empty capillary.

- [1] a) H. Schmidbaur, A. Schier, *Chem. Soc. Rev.* **2008**, *37*, 1931–1951; b) H. Schmidbaur (Ed.) *Gold: Progress in Chemistry, Biochemistry and Technology*, Wiley, **1999**.
- [2] a) H. Schmidbaur *Gold Bull.* **2000**, *33*, 3–10; b) R. J. Puddephatt, *The Chemistry of Gold*, Elsevier, Amsterdam, **1978**.
- [3] a) M. J. Katz, K. Sakai, D. B. Leznoff, *Chem. Soc. Rev.* **2008**, *37*, 2012–2027.
- [4] R. E. Bachman, M. S. Fioritto, S. K. Fetics, T. M. Cocker, *J. Am. Chem. Soc.* **2001**, *123*, 5376–5377.
- [5] a) E. R. T. Teikink, J. G. Kang, *Coord. Chem. Rev.* **2009**, *253*, 1627–1648; b) V. W.-W. Yam, E. C.-C. Cheng, *Chem. Soc. Rev.* **2008**, *37*, 1806–1813; c) J. M. Forward, D. Bohmann, J. P. Fackler, Jr., R. J. Staples, *Inorg. Chem.* **1995**, *34*, 6330–6336.
- [6] a) A. S. K. Hashmi, M. Rudolph, *Chem. Soc. Rev.* **2008**, *37*, 1766–1775; b) M. Chen, D. W. Goodman, *Chem. Soc. Rev.* **2008**, *37*, 1860–1870; c) C. D. Pina, E. Falletta, L. Prati, M. Rossi, *Chem. Soc. Rev.* **2008**, *37*, 2077–2095.
- [7] a) M. J. Katz, T. Ramnial, H. Z. Hu, D. B. Leznoff, *J. Am. Chem. Soc.* **2008**, *130*, 10662–10673; b) E. J. Fernandez, J. M. Lopez de Luzuriaga, M. M. Monge, M. Montiel, M. E. Olmos, J. Perez, A. Laguna, F. Mendiabal, A. A. Mohamed, J. P. Fackler, Jr., *Inorg. Chem.* **2004**, *43*, 3573–3581.
- [8] a) S. Ahman, A. A. Isab, S. Ali, A. R. Al-Arfaj, *Polyhedron* **2006**, *25*, 1633–1645; b) A. A. Mohamed, H. E. Abdou, J. Chen, A. E. Bruce, M. R. M. Bruce, *Comment Inorg. Chem.* **2002**, *23*, 321–334.
- [9] P. T. Bishop, *Gold Bull.* **2002**, *35*, 89–98.
- [10] a) G. Heimel, L. Romaner, J. L. Bredas, E. Zojer, *Langmuir* **2008**, *24*, 474–482; b) A. Ulman, *Acc. Chem. Res.* **2001**, *34*, 855–863; c) J. B. Schlenoff, M. Li, H. Ly, *J. Am. Chem. Soc.* **1995**, *117*, 12528–12536.
- [11] a) I. Dolamic, C. Gautier, J. Boudon, N. Shalkevich, T. Burgi, *J. Phys. Chem. C* **2008**, *112*, 5816–5824; b) A. R. Tao, S. Habas, P. D. Yang, *Small* **2008**, *4*, 310–325; c) C. N. R. Rao, G. U. Kulkani, P. J. Thomas, P. P. Edwards, *Chem. Soc. Rev.* **2000**, *29*, 37–35.
- [12] M. Brust, M. Walker, D. Bethell, D. J. Schiffrin, R. Whyman, C. Kiely, *J. Chem. Soc., Chem. Commun.* **1994**, 801–803.
- [13] R. E. Bachman, S. A. Bodolosky-Bettis, S. C. Glennon, S. A. Sirchio, *J. Am. Chem. Soc.* **2000**, *122*, 7146–7147.
- [14] a) S.-H. Cha, J.-U. Kim, K.-H. Kim, J.-C. Lee, *Chem. Mater.* **2007**, *19*, 6297–6303; b) J. D. E. T. Wilton-Ely, H. Ehlich, A. Schier, H. Schmidbaur, *Helv. Chim. Acta* **2001**, *84*, 3216–3232; c) R. P. Brinas, M. Hu, L. Qian, E. S. Lymar, J. F. Hainfeld, *J. Am. Chem. Soc.* **2008**, *130*, 975–982.
- [15] R. E. Bachman, S. A. Bodolosky-Bettis, C. M. Pyle, M. A. Gray, *J. Am. Chem. Soc.* **2008**, *130*, 14303–14310.
- [16] A. K. H. A-Saady, K. Moss, C. A. McAuliffe, R. V. Parish, *J. Chem. Soc., Dalton Trans.* **1984**, 1609–1616.
- [17] a) W. Schneider, A. Bauer, H. Schmidbaur, *Organometallics*, **1996**, *15*, 5445–5446; b) J. D. E. T. Wilton-Ely, A. Schier, H. Schmidbaur, *Organometallics*, **2001**, *20*, 1895–1897.
- [18] a) Z. Assefa, B. G. McBurnett, R. J. Staples, J. P. Fackler, Jr., B. Assmann, K. Angermair, H. Schmidbaur, *Inorg. Chem.* **1995**, *34*, 75–83; b) Z. Assefa, B. G. McBurnett, R. J. Staples, J. P. Fackler, Jr., *Inorg. Chem.* **1995**, *34*, 4965–4972; c) W. B. Jones, J. Yuan, R. Narayanaswamy, M. A. Young, R. C. Elder, A. E. Bruce, M. R. M. Bruce, *Inorg. Chem.* **1995**, *34*, 1996–2001; d) J. M. Forward, D. Bohmann, J. P. Fackler, Jr., R. J. Staples, *Inorg. Chem.* **1995**, *34*, 6330–6336; e) C. King, J.-C. Wang, M. N. I. Khan, J. P. Fackler, Jr., *Inorg. Chem.* **1989**, *28*, 2145–2149.
- [19] V. R. Thalladi, H.-C. Weiss, D. Bläser, R. Boese, A. Nangia, G. R. Desiraju, *J. Am. Chem. Soc.* **1998**, *120*, 8702–8710.
- [20] a) G. W. Gokel, R. P. Wiedera, W. P. Weber, *Org. Synth.* **1975**, *55*, 96–99; b) W. Schneider, K. Angermaier, A. Sladek, H. Schmidbaur, *Z. Naturforsch.* **1996**, *51b*, 790–800.
- [21] a) R. H. Blessing, *Acta Crystallogr.* **1995**, *A51*, 33–38; b) G. M. Sheldrick, SADABS, Program for Empirical Absorption Correction of Area Detector Data, University of Göttingen, Göttingen (Germany) **1996**.
- [22] G. M. Sheldrick, SHELXTL (version 5.10), Bruker Analytical X-ray Instruments Inc., Madison, Wisconsin (USA) **1998**.
- [23] L. J. Barbour, X-SEED, A software tool for supramolecular crystallography, University of Stellenbosch, Stellenbosch (South Africa) **1999**. See also: L. J. Barbour, *J. Supramol. Chem.* **2001**, *1*, 189–191.